ACS APPLIED MATERIALS & INTERFACES

Research Article

www.acsami.org

Increased Bioavailability of Rifampicin from Stimuli-Responsive Smart Nano Carrier

Shivshankar R. Mane,[†] Himadri Dinda,[†] Ashlin Sathyan,[†] Jayasri Das Sarma,[‡] and Raja Shunmugam*[,†]

[†]Polymer Research Centre, Department of Chemical Sciences and [‡]Department of Biological Sciences, Indian Institute of Science Education and Research Kolkata (IISER K), Haringhata, West Bengal, India

Supporting Information

ABSTRACT: Stimuli responsive polymeric nanocarrier (**RCOP-2**) functionalized with frontline antituberculosis drug (Rifampicin) is demonstrated for sustained release. Bioavailability of Rifampicin is taken care of by conjugating this drug through a acylhydrazine linker to the polymeric backbone. The poly(ethylene glycol) structural motif is introduced in the copolymer architecture for water solubility. Releasing retinal along with Rifampicin is hypothesized to reduce the risk of side effects due to Rifampicin. The self-assembly of **RCOP-2**, due to the amphiphilicity present in the copolymer, is explored in detail. The pH responsiveness of **RCOP-2** is demonstrated in mild acidic environment as well as in cell lines. The 4T cell line, due to its acidic nature, shows time-dependent cellular internalization. On the basis of the results, our unique design is expected to provide an increased bioavalaibility of Rifampicin with reduced side effects. From the flow cytometry results on A549 cell lines, it is clear that the newly designed copolymer **RCOP-2** can internalize efficiently and serve as an effective Rifampicin delivery system.

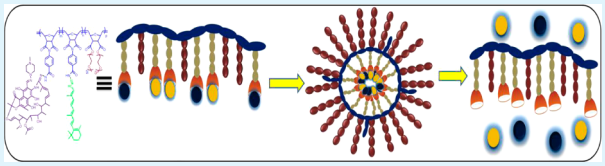

KEYWORDS: *drug delivery, Rifampicin, retinal, ROMP, stimuli responsive*

INTRODUCTION

Tuberculosis (TB) is one of most common causes of death.[1] Recently, the use of multidrug regimens having Rifampicin (**RIF**), along with other frontline drugs, is employed for the treatment of TB.[2] There are some reports on the delivery of frontline antituberculosis drugs **RIF** and isoniazid (**INZ**) using different delivery systems such as liposomes and microspheres.[3] These systems have demonstrated little chemotherapeutic efficacy, but they have failed in releasing the drugs in a controlled and sustained fashion. Most importantly, these existing polymeric carriers are not available for releasing **RIF** without losing its bioavailability.[1−4] Recently, Zhuang et.al have reported the encapsulation of **RIF** in polymeric micellar system;[5] but the problem associated with **RIF** is that it decomposes rapidly at pH 1−3 (stomach)[6] (Supporting Information, Scheme S1). During this process, the **RIF** drug gets decomposed before it kills the bacteria (TB cell). So the noncovalent approach is not helpful in this case. The success of the treatment, which depends on the good bioavailability leading to adequate plasma and tissue concentration of **RIF**, is absolutely mandatory. Moreover, the long time intake of frontline anti-TB drug may be a cause for several diseases. These are nausea, headache, and drowsiness as well as eye defects such as optic neuritis and icterus, which, when caused by the frontline antituberculosis drugs **INZ** and **RIF**, have been ignored.[7,8] So the challenges in the field of antituberculosis therapy are (1) to develop a controlled and sustained drug delivery system, (2) to make bioavailability of the **RIF** drug, (3) to reduce side effects, especially on eyes, and (4) to enhance blood circulation times. To address these challenges, an ideal system needs to be designed, which should show high efficacy of the drugs along with the physicochemical properties like water solubility, pH range, biocompatibility, and bioavailability.[9−15]

Toward this end, we designed a copolymer **RCOP-2** (**polyRIF-RET-PEG**), an ideal drug delivery system that is potentially expected to impart the controlled/sustained drug release, bioavailability of the drug, prolonged circulation time, and reduced side effects. The **RIF** is conjugated along with retinal (**RET**), which is primarily to overcome the eye defects caused by the drugs. Poly(ethylene glycol) (**PEG**) is added in the design to provide biocompatibility and prolonged circulation time. The copolymer **RCOP-2** is prepared by using ring-opening metathesis polymerization (ROMP) technique. **RCOP-2** is designed in such a way that both **RIF** and **RET** are attached to norbornene backbone through acylhydrazine linker so that it shall be released under mild acidic conditions. Because of the huge amphiphilicity present in the copolymer structure, **RCOP-2** is expected to self-assemble into nanocarriers under the aqueous conditions. The hydrophobic core of this nanocarrier contains **RIF** and **RET** motifs, whereas the hydrophilic shell is decorated with **PEG** functionality. This structure also plays an important role in keeping the bioavailability of **RIF** by not exposing it to the acidic environment. The hydrophilic shell structure provides drug resistance by hiding cytotoxic drugs in the carrier. The

Received: July 8, 2014
Accepted: September 9, 2014
Published: September 9, 2014

stimuli responsive acylhydrazine linker provides significant release of the drugs under acidic environment such as *Mycobacterium smegmatis*-containing phagosomes (pH 4.7−5.5).[16] The MTT assay against 4T cell line shows significant inhibition in cell growth. This report efficiently demonstrates the attachment of the structurally very complex frontline antitubercular drug **RIF** and retinal (vitamin A) molecules to norbornene monomer and the subsequent polymerization of this monomer in a controlled fashion to produce effective drug delivery system.

EXPERIMENTAL SECTION

A complete list of chemicals,[17] the techniques to characterize all the polymers,[23,24] and a detailed experimental procedure[17,18] to make the monomers as well as polymers, is discussed in the Supporting Information.

RESULT AND DISCUSSION

A nanocarrier-based drug delivery vehicle to release **RIF** along with retinal is proposed in the manuscript. Toward this end, three norbornene-derived monomers, namely, **Mono 1−3**, were first synthesized[17,18] and thoroughly characterized by FT-IR, ^{1}H, and ^{13}C NMR spectroscopy techniques (Supporting Information, Scheme S2 and Figures S1−S8). The detailed synthetic procedure as well as characterization of molecules **1** to **3** along with all monomers is discussed under the Experimental Section of the Supporting Information. Having confirmed the successful formation of all three monomers, the polymerization kinetics for **Mono 1** and **Mono 2** were explored. Because of the functional group tolerance of Grubbs' catalyst, the ring-opening metathesis polymerization (ROMP) technique was used for the preparation of monodisperse polymeric prodrugs.[19−24] It was mandatory to study the polymerization kinetics of each monomer as they would eventually be used to make well-controlled copolymers. Hence, the homopolymerization kinetics were explored for **Mono 1−3** (Supporting Information, Schemes S3 and S4).

The polymerization kinetics was monitored through ^{1}H NMR spectroscopy and gel permeation chromatography (GPC) techniques. The molecular weight was measured using polystyrene as a standard. From the kinetics study, it was clear that **Mono 1−3** were polymerized in a very controlled fashion and produced **RIF-P1−5**, **RET-P1−5**, and **PEG-P1−5** homopolymer with narrow polydispersity index (PDI) (Figure 1a,b and Supporting Information, Figures S11−S14). It was also surprising to observe that the target M_w was almost achieved in all polymers despite the complexity of the monomer functionality (Table 1 and Supporting Information, Table S1). After carefully monitoring the homopolymerization kinetics of all the monomers, the copolymerization was explored. For the copolymerization, different sets of copolymers **CP-1** (**polyRET-PEG**), **CP-2** (**polyRIF-PEG**), **RCOP-1** (**polyRIF-RET**), and **RCOP-2** (**polyRIF-RET-PEG**) were prepared from **Mono 1−3** by using second generation Grubbs' catalyst. The detailed synthetic procedures and complete characterizations are given in the Experimental Section of the Supporting Information. The polymerization reaction was monitorred using ^{1}H NMR spectroscopy and the GPC technique. The formation of **RCOP-1** was confirmed by the disappearance of norbornene olefinic proton signal at δ 6.5 ppm and by the appearance of one new signal at δ 5.2 ppm along with respective protons signals for **RIF** as well as retinal (Supporting Information, Figure S9). The **RCOP-1** was only

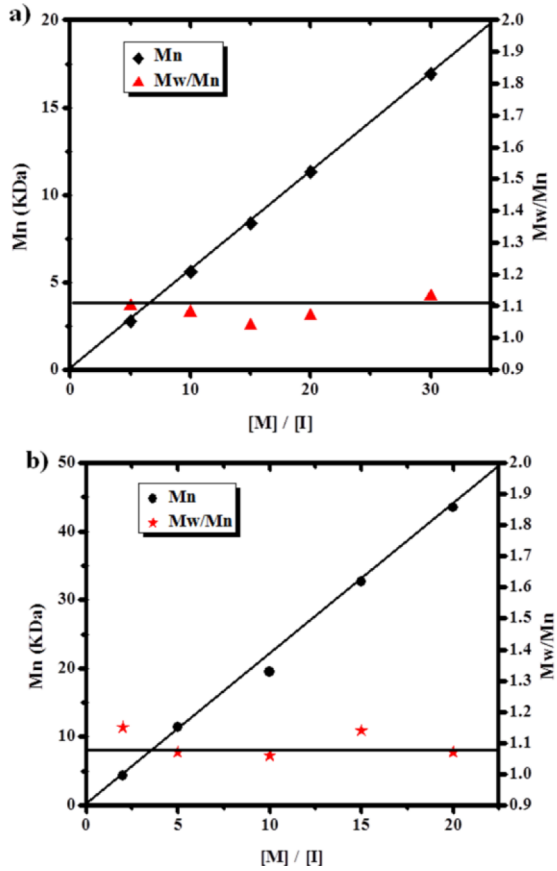

Figure 1. (a) Plot of M_n vs [M]/[I] for **RET-P1−5**. (b) Plot of M_n vs [M]/[I] for **PEG-P1−5**.

soluble in organic solvent. To make the water-soluble prodrug, PEG containing **Mono 3** was introduced to get new copolymer **RCOP-2** (Scheme 1). The formation of **RCOP-2** was confirmed by ^{1}H NMR spectroscopy and GPC technique. In the ^{1}H NMR spectroscopy, the disappearance of the signal at δ 6.5 ppm and appearance of new signal at δ 5.29 ppm along with the signals at δ 3.57−3.89 ppm (responsible for PEG motif) confirmed the formation of **RCOP-2** (Supporting Information, Figure S10). The molecular weight of the copolymer was measured using polystyrene standard. The observed molecular weight for **RCOP-1** was M_n = 12 100 with PDI = 1.12 (Figure 2a), and for **RCOP-2**, it was M_n = 22 400 with PDI = 1.08 (Figure 2b). It was observed that all the polymers had very well-controlled molecular weights with narrow PDI. The composition for **RCOP-1** was **Mono 1**/**Mono 2** (1:1 mol equiv), and the composition for **RCOP-2** was **Mono 1**/**Mono 2**/**Mono 3** (1:1:2 mol equiv), respectively. The composition for control molecules copolymer **CP-1** was **Mono 2**/**Mono 3** (1:1 mol equiv) and **CP-2** was **Mono 1**/**Mono 3** (1:1 mol equiv). In the **RCOP-2** copolymer, the percentage of **RET** as well as **RIF** was about 18.34% and 12.67%, respectively.

After the successful synthesis of copolymer **RCOP-2**, the aggregation behavior of **RCOP-2** was tested in aqueous condition. The aggregation of **RCOP-2** was expected in polar solvent due to its obvious amphiphilicity. Critical micellar contentration (CMC) was studied to confirm the formation of aggregation. To study CMC, pyrene was used as a hydrophobic probe. The concentration of pyrene was maintained at 0.2 μM, and the concentration of **RCOP-2** was varied from 0.001 to 300 μg mL^{-1}. The CMC was measured using fluorescence

Table 1. Homopolymerization Kinetics for RET and PEG Monomers

RET homopolymer P1–P5					PEG homopolymer P1–P5				
polymers	[M]/[I]	M_n[a]	M_n[b]	PDI[c]	polymers	[M]/[I]	M_n[a]	M_n[b]	PDI[c]
P1	5:1	2825	2600	1.10	P1	2:1	4600	4300	1.15
P2	10:1	5650	5400	1.08	P2	5:1	11 500	11 400	1.07
P3	15:1	8475	6300	1.04	P3	10:1	23 000	19 500	1.06
P4	20:1	11 300	9900	1.07	P4	15:1	34 500	32 600	1.14
P5	30:1	16 950	14 600	1.13	P5	20:1	46 000	43 500	1.07

[a]Target molecular weight of the polymer. [b]Molecular weight by GPC. [c]Ratio of weight-average molecular weight by number-average molecular weight.

Scheme 1. Synthesis of polyRIF-RET-PEG (RCOP-2) Copolymer via ROMP

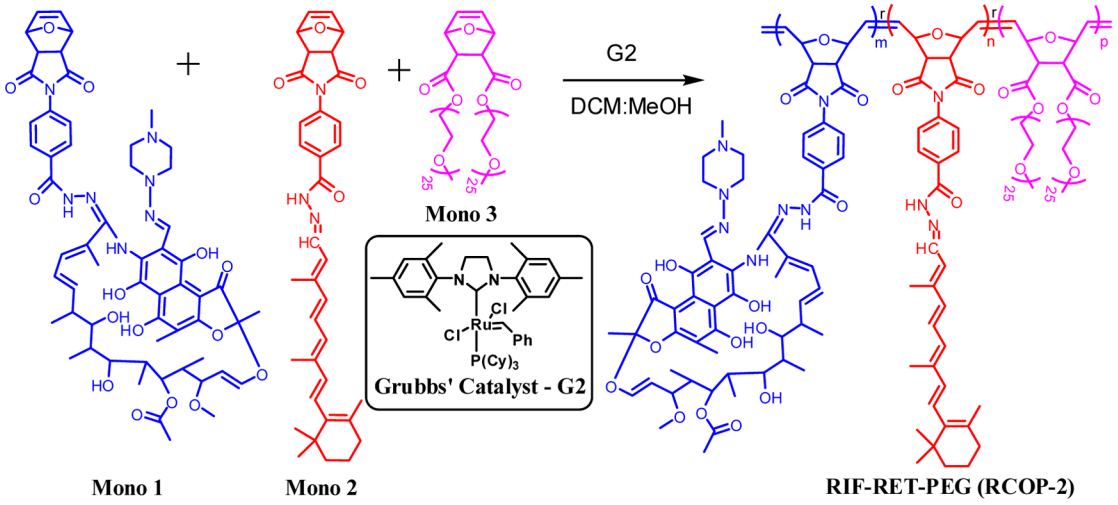

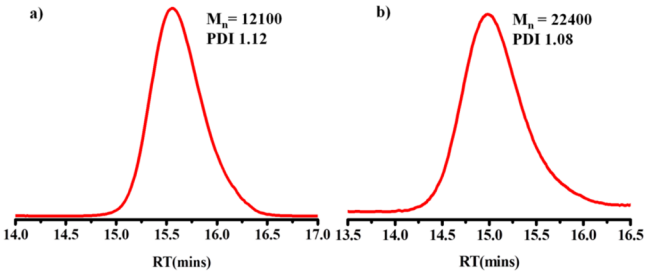

Figure 2. GPC traces for (a) **RCOP-1** and (b) **RCOP-2**.

spectroscopy; with the excitation wavelength set at 339 nm, the emission intensities were monitored at 371, 382, and 391 nm. The relative intensities I_{391}/I_{371} were varried as a function of **RCOP-2** concentration. The CMC was observed as 56 μg mL^{-1} (Supporting Information, Figure S15). From CMC studies, it was clear that **RCOP-2** forms aggregates under aqueous conditions. To ensure this, the hydrodynamic radius was measured using dynamic light scattering (DLS) in aqueous environment. The observed size of **RCOP-2** was 106 nm with 0.14 PDI (Figure 3a). Furthermore, the morphology of **RCOP-2** aggregates was studied using atomic force microscope (AFM), scanning electron microscopy (SEM), and transmission electron microscopy (TEM). The **RCOP-2** aggregates showed a spherical shape by AFM (Figure 3b), SEM (Figure 3c), and TEM (Figure 3d). It was interesting to note that the size of the **RCOP-2** aggregates from all three microscopies (about 100 nm), which was in good agreement with the DLS data. The overall self-assembly processs of **RCOP-2** was demonstrated by a cartoon representation in Figure 3e.

On the basis of the morphological studies, it was evident that the new copolymer, **RCOP-2**, aggregated as a spherical nanocarrier under aqueous conditions. To prove the reservoir capabilities of the newly designed nanocarrier, the sustained release experiments were explored. Toward this end, the pH conditions in *Mycobacterium tuberculosis* and *M. smegmatis* was analyzed. It was observed from the literature that the pH in the *M. smegmetis*-containing phagosomes was in range of 4.7–5.5.[16,25,26] Therefore, the in vitro drug release profile of **RCOP-2** was evaluated in physiological pH as well as mycobacterium in macrophage compartments pH 5.5. For the triggered release, the solution of 1 mg of **RCOP-2** in water was loaded in a dialysis tube (3500 Da cutoff). The **RCOP-2** prodrug was dialyzed against buffer solution whose pH was maintained at 5.5 and 7.4. Both the **RIF** and retinal were conjugated through acylhydrazine linker. It was expected that the same drug-release kinetics would be achieved under acidic environment. The drug-release kinetics of **RIF** as well as retinal was monitored by UV spectroscopy. The absorbance at 470 and 330 nm were responsible for **RIF** and retinal, respectively (Figure 4a). It was observed that at pH 7.4, there was no significant release of drug from **RCOP-2** (less than 2%). This indicated the stability of **RCOP-2** under physiological condition. At pH 5.5, a maximum drug release was observed at about 61% (for retinal) and 45% (for **RIF**) as shown in Figure 4b. This result indicated the importance of acylhydrazine linker. This demonstrated the feasibility of potential drug delivery in macrophage compartments. The overall self-assembly process of **RCOP-2** and its stimuli responsiveness were demonstrated by cartoon representation (Figure 4c).

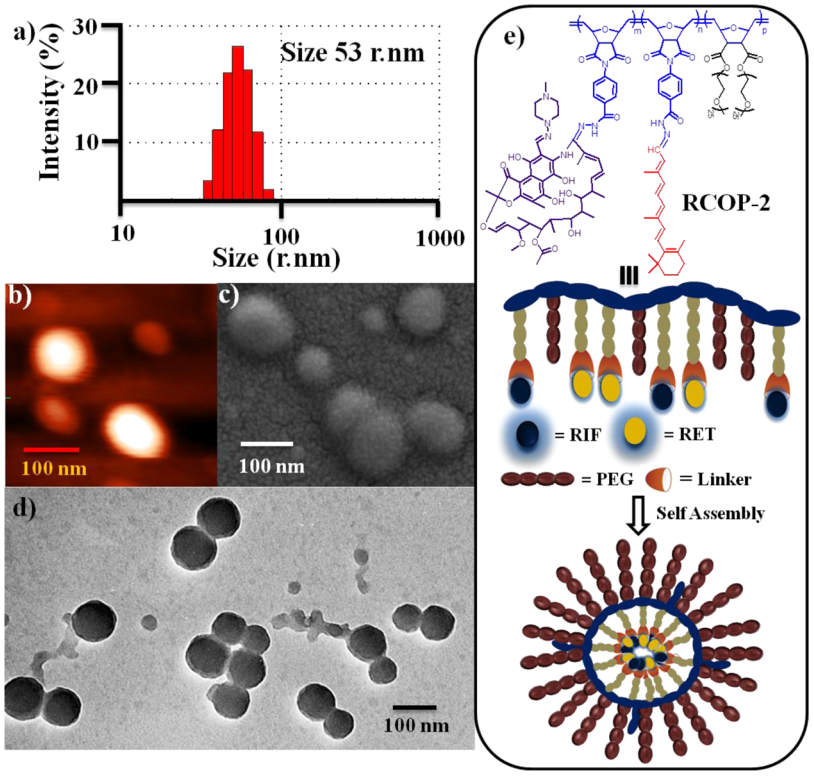

Figure 3. Characterization of self-assembled aggregates from **RCOP-2**; (a) DLS data; (b) representative image of **RCOP-2** from AFM analysis; (c) SEM image of **RCOP-2**; (d) TEM image; (e) cartoon representation for overall self-assembly process of **RCOP-2** in aqueous environment.

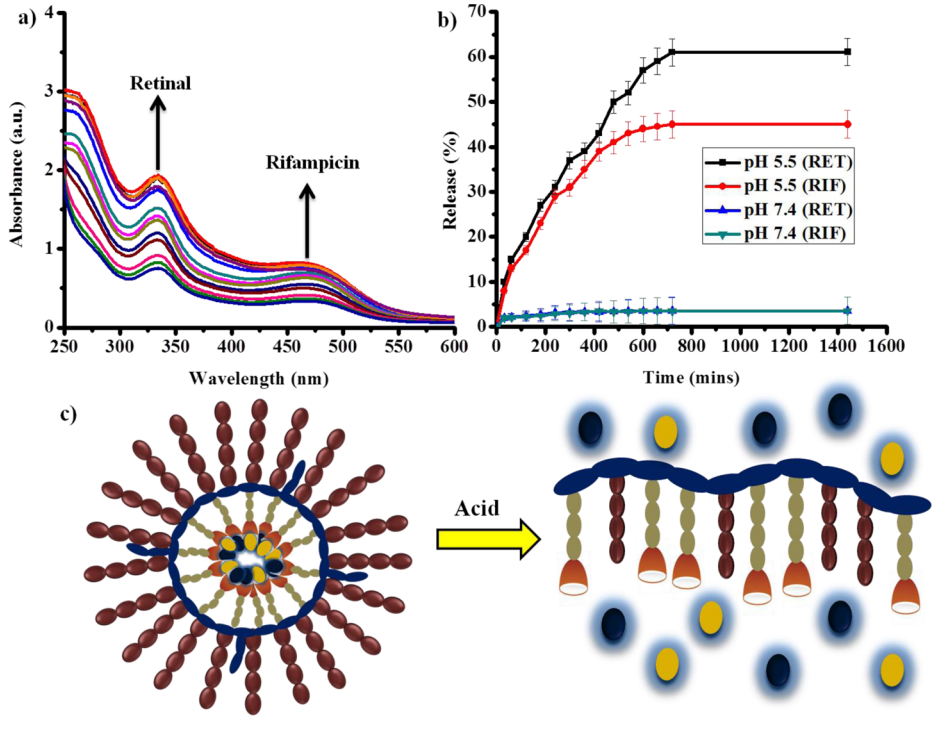

Figure 4. (a) UV spectra for the drug release at pH 5.5. (b) Cumulative drug release profile for **RCOP-2**. (c) A cartoon representation for drug release from the self-assembly of **RCOP-2**.

Motivated with the biocompatible and renal clearance results on norbornene systems,[18,27] we explored the cell viability and cell uptake of the newly designed nanocarrier. The effect of **RCOP-2** on the cell viability was monitored by MTT assay. The cell viability was evaluated by incubating the cells with increasing concentration (1 to 1000 μg/mL) up to 72 h, after which the viability of the cell was determined. The effective cleavage of drug and biocompatibility studies were performed on 4T cell lines as well as A549 cell lines (Figure 5). It was observed that the 4T cell showed cytotoxic effect from 5 μg/

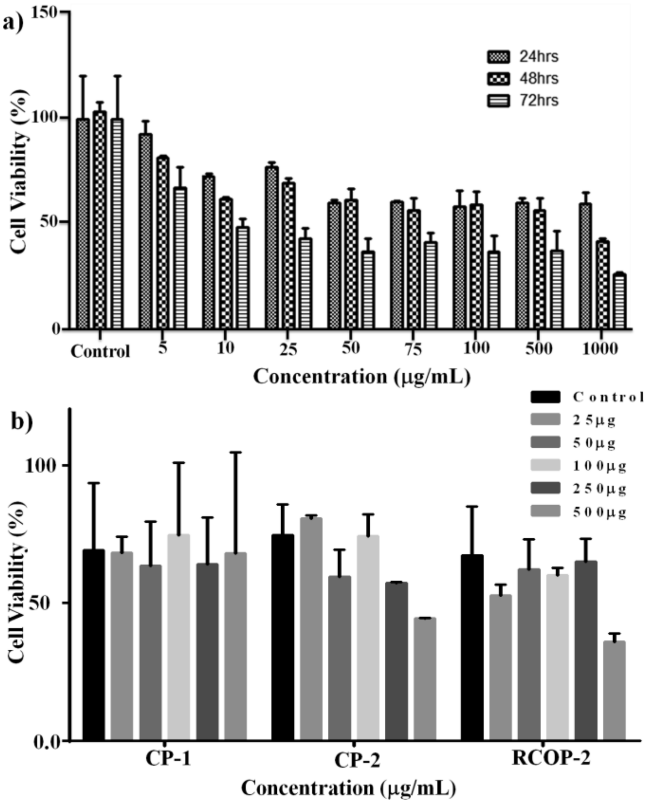

Figure 5. Cytotoxicity profile of **RCOP-2** in (a) 4T cell line and in (b) A549 cell line (72 h).

mL concentration onward. Approximately 50% cell death was observed at ~100 μg/mL concentration (Figure 5a). Surprisingly, the cytotoxic effect of **RCOP-2** on 4T cell line showed a highly toxic effect. Also **RCOP-2** showed cytotoxic effect on A549 cell line (Figure 5b and Supporting Information, Figures S18 and S19). From this study, it was clear that the combination of **RCOP-2** showed highly toxic effect as compared to monomeric **RIF**. Similarly, the cell viability of monomers was determined as described in Supporting Information (Figures S16 and S17).

The most frequently used alveolar epithelial model, namely, the A549 cell line (due to its morphological and biochemical features of the human pulmonary alveolar type II cell in situ), was chosen as model cell line to demonstrate the pulmanory drug delivery.[14,15] Since the nanocarrier could generate fluorescence emission in orange and green spectrum due to retinal and **RIF**, respectively, fluorescence channels, namely, V450 (excitation 405 nm, emission 425.5−470.5 nm) and FITC (excitation 488 nm, emission 511−543 nm) were chosen for **CP-1**, **CP-2**, and **ROCP-2** molecules (Figures 6−9 and Supporting Information, Figures S20−S23).

To analyze the fluorescence activated cell sorting results in side scatter channel (SSC) versus forward scatter channel (FSC), dot plot "P1" gate was kept to sort out the desired cell population for further analysis. The P1 gate was first applied in the case of SSC versus FITC dot plot for **RIF**, then for SSC versus V450 dot plot for retinal, and finally in the case of FITC as well as V450 histogram. "P2" gate for **RIF** and "P3" gate for retinal were kept to get the mean fluorescence intensity (MFI) of that initially gated cell population P1. MFI values for the control tubes were observed as 18 558 and 14 445 in FITC

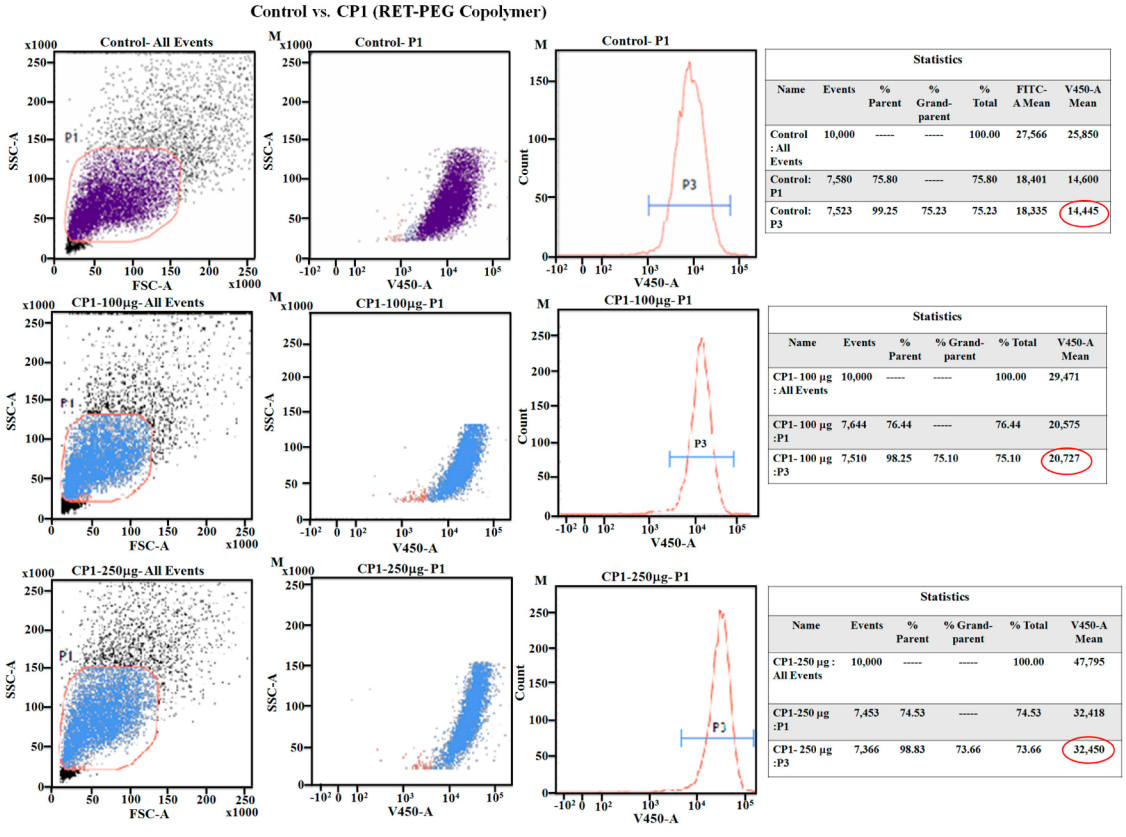

Figure 6. Cell viability data from flow cytometry (FITC-FL study) of **CP-1** (**polyRET-PEG**).

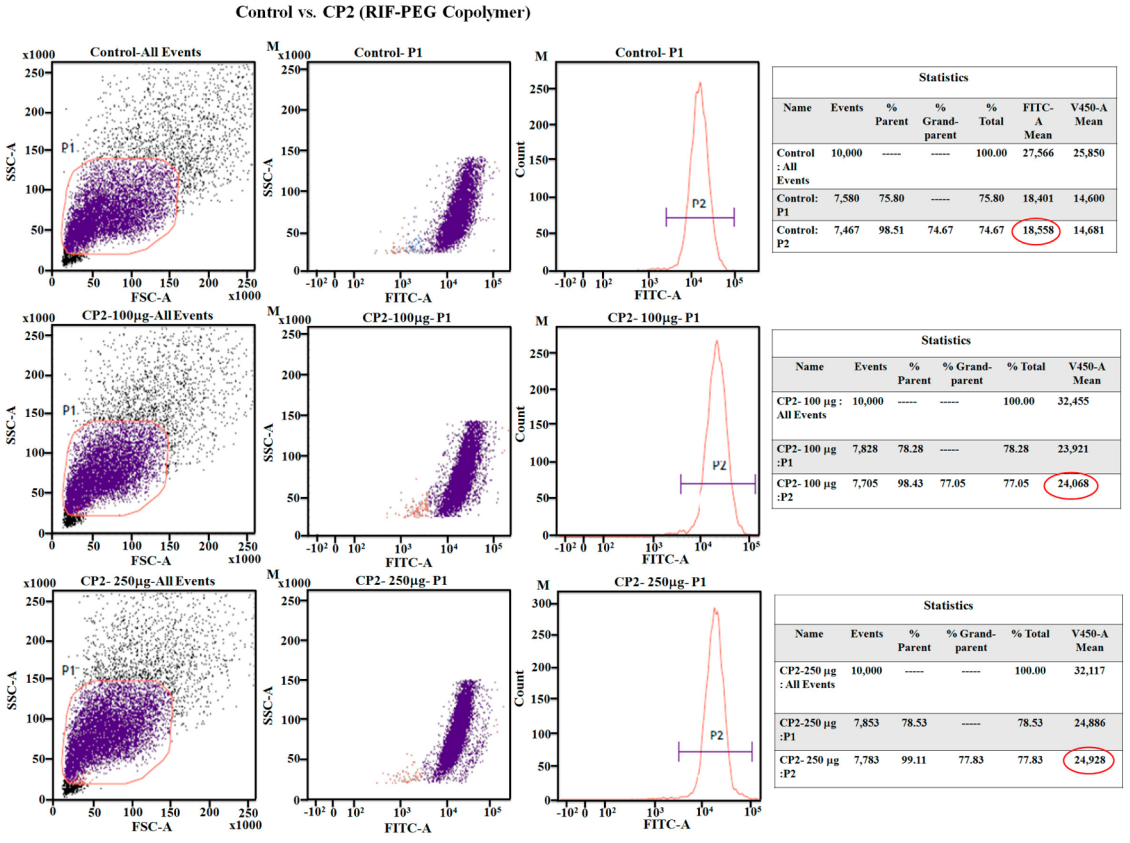

Figure 7. Cell viability data from flow cytometry (FITC-FL study) of **CP-2** (**polyRIF-PEG**).

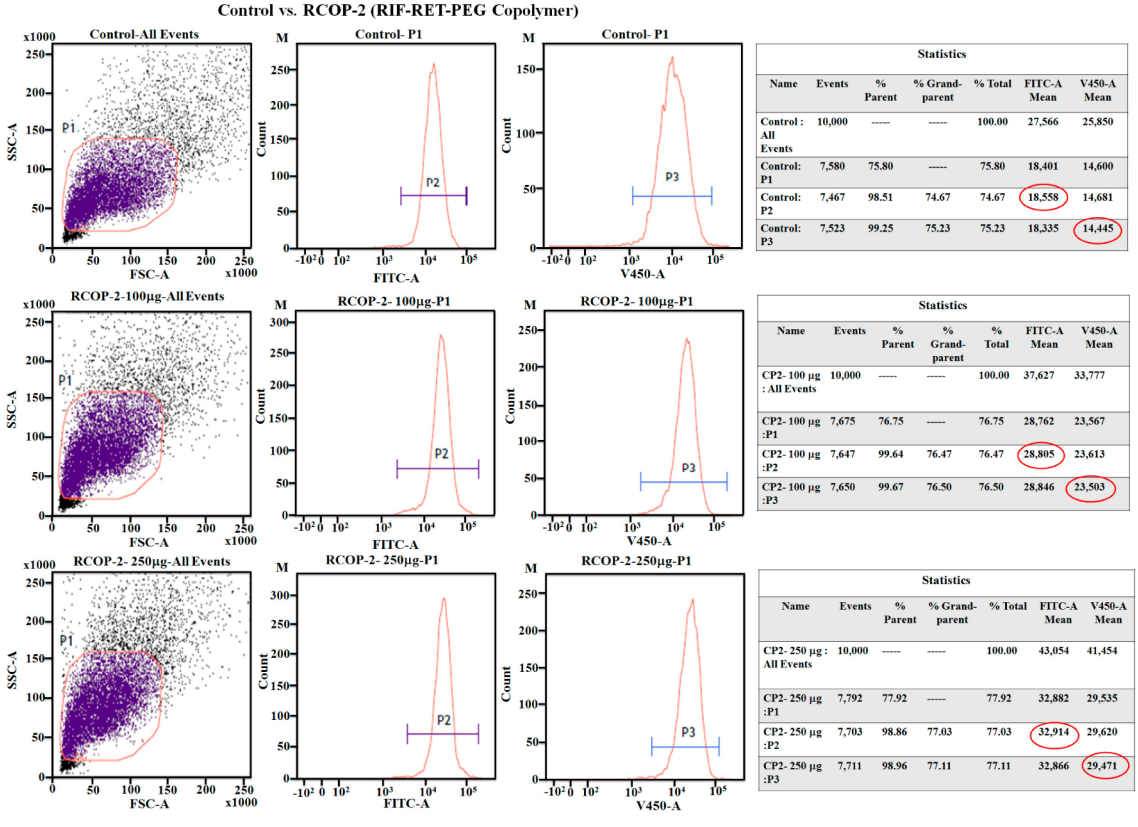

Figure 8. Cell viability data from flow cytometry (FITC-FL study) of **RCOP-2**.

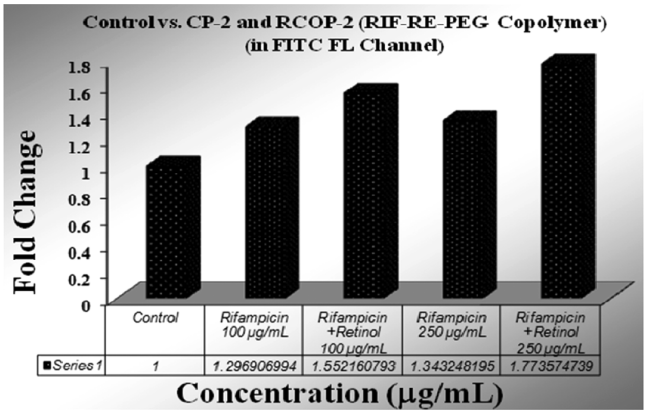

Figure 9. FITC-FL study of **RCOP-2** (excitation 488 nm, emission 511−543 nm).

channel and V450 channel, respectively, due to the primary PMT voltage (FSC 101.3 mV, threshold FSC 10 000, SSC 286.4 mV, FITC 306.5 mV, V450−308.1 mV). Subsequently, **CP-1** (100 μg/mL) and **CP-1** (250 μg/mL) tubes gave 20 727 and 32 450 MFI values, respectively (Figure 6). Similarly, MFI values for **CP-2** (100 μg/mL) and **CP-2** (250 μg/mL) tubes were observed as 24 068 and 24 928, respectively (Figure 7). Interestingly, **RCOP-2** (100 μg/mL) and **RCOP-2** (250 μg/mL) showed values of 28 805 and 32 914, respectively, in FITC channel (corresponding MFI values were 23 503 and 29471, respectively) (Figure 8). All these tubes exerted high MFI value and true positive signal due to fluorescence emission. Therefore, the presence of **CP-2** and conjugation of **RCOP-2** molecules exerted MFI value approximately 1.29-fold and 1.55-fold, respectively (in 100 μg/mL concentration), compared to the control molecule. Similarly, the MFI values were approximately 1.34-fold and 1.77-fold, respectively (in 250 μg/mL concentration), with respect to the control molecule. From these studies it was clearly evident that internalization as well as efficiency was greater in the case of **RCOP-2** compared to the control molecules (Figure 9).

Finally, to study the cellular internalization property, the nanocarrier **RCOP-2** was incubated in 4T cell line. Epifluorescence microscope images indicated that these **RCOP-2** nanocarriers were easily internalized by the living cell (Figure 10). From the epifluorescence microscope image, it was clear that, with respect to increasing time, the nanocarrier **RCOP-2** efficiently entered into the cell and released both the drug and retinal in acidic environment. The green color was observed around the nucleus due to **RIF**. The photoluminescence spectra of **RCOP-2** are given in Supporting Information (Figure S24). The effect of **RCOP-2** on cell growth and cell division prompted us to propose the stimuli responsive nanocarrier. Testing of the efficacy of **RCOP-2** on TB-affected cell lines is in progress, and it will be our future report.

CONCLUSIONS

Here we have demonstrated a facile approach to achieve the bioavailability of **RIF** by conjugating it to the norbornene using acylhydrazine linker. ROMP, a controlled polymerization technique, is used to prepare copolymer of norbornene-derived **RIF** along with **RET** and **PEG** monomers. Retinal is released along with **RIF** from the **RCOP-2** copolymer to reduce the side effects on eyes due to the frontline anti-TB drugs. CMC and

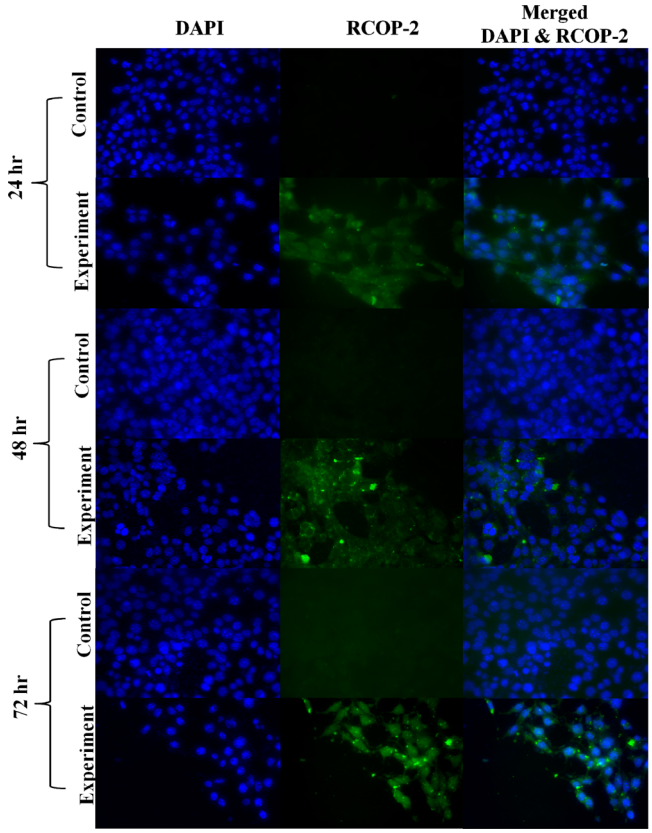

Figure 10. Epifluorescence pictures for the uptake of **RCOP-2** in 4T cells. Cells were plated on coverslips inserted into 24-well tissue culture plates. Confluent monolayer cells were loaded with 100 μg/mL of **RCOP-2** at 72 h.

DLS studies confirm the formation of aggregates. The observed CMC is 56 μg/mL, and the size of aggregates by DLS is 106 nm. The spherical nature of the aggregates is confirmed by AFM, TEM, and SEM analysis. The stimuli responsive nature of **RCOP-2** is evaluated under acidic environment. Dialysis study reveals the stability of **RCOP-2** in extracellular conditions and is not stable at microphage compartment pH (4.7−5.5). The MTT assay against 4T cell line shows the high cytotoxicity with lower concentration of **RCOP-2**. Furthermore, the cellular uptake study on 4T cell line has demonstrated that the nanocarrier **RCOP-2** is easily internalized by the living cell. On the basis of the flow cytometry experimental evidence on A549 cell lines, it is clear that the newly designed copolymer **RCOP-2** can be internalized efficiently and serve as an effective **RIF** delivery system.

ASSOCIATED CONTENT

Supporting Information

Synthesis Schemes S1−S4, Materials and Methods, Experimental Procedure for the synthesis of **Mono 1−3**, copolymerization procedure, complete characterization of monomers, and additional analytical data. This material is available free of charge via the Internet at http://pubs.acs.org.

AUTHOR INFORMATION

Corresponding Author

*E-mail: sraja@iiserkol.ac.in. (R.S.)

Notes

The authors declare no competing financial interest.

■ ACKNOWLEDGMENTS

S.R.M. thanks CSIR, New Delhi, for research fellowship. R.S. and H.D. thank DST, New Delhi, for Ramanujan Fellowship. R.S. and J.D.S. thank IISER-Kolkata for the infrastructure and start-up funding.

■ REFERENCES

(1) Patton, J. S. Mechanisms of Macromolecule Absorption by the Lungs. *Adv. Drug Delivery Rev.* **1996**, *19*, 3−36.
(2) Patton, J. S.; Fishburn, C. S.; Weers, J. G. The Lungs as a Portal of Entry for Systemic Drug Delivery. *Proc. Am. Thorac. Soc.* **2004**, *1*, 338−344.
(3) Ferebee, S. H. Controlled Chemoprophylaxis Trials in *Tuberculosis*: a General Review. *Adv. Tuberc. Res.* **1970**, *17*, 28−106.
(4) Ulbrich, K.; Subr, V. Polymeric Anticancer Drugs with pH-Controlled Activation. *Adv. Drug Delivery Rev.* **2004**, *56*, 1023−1050.
(5) Wang, W.; Ding, J.; Xiao, C.; Tang, Z.; Li, D.; Chen, J.; Zhuang, X.; Chen, X. Synthesis of Amphiphilic Alternating Polyesters with Oligo(ethylene glycol) Side Chains and Potential Use for Sustained Release Drug Delivery. *Biomacromolecules* **2011**, *12*, 2466−2474.
(6) Singh, S.; Mariappan, T. T.; Sharda, N.; Kumar, S.; Chakraborti, A. K. The Reason for an Increase in Decomposition of Rifampicin in the Presence of Isoniazid Under Acid Conditions. *Pharm. Pharmacol. Commun.* **2000**, *6*, 405−410.
(7) Zhang, Y.; Amzel, L. M. Tuberculosis Drug Targets. *Curr. Drug Targets* **2002**, *3*, 131−154.
(8) Zhang, Y.; Post-Martens, K.; Denkin, S. New Drug Candidates and Therapeutic Targets for Tuberculosis Therapy. *Drug Discovery Today* **2006**, *11*, 21−27.
(9) Patton, J. S.; Byron, P. R. Inhaling Medicines: Delivering Drugs to the Body Through the Lungs. *Nat. Rev. Drug Discovery* **2007**, *6*, 67−74.
(10) Hamman, J. H.; Gill, M. E.; Awie, F. K. Oral Delivery of Peptide Drugs: Barriers and Developments. *BioDrugs* **2005**, *19*, 165−177.
(11) Chellat, F.; Merhi, Y.; Moreau, A.; Yahia, L. Therapeutic Potential of Nanoparticulate Systems for Macrophage Targeting. *Biomaterials* **2005**, *26*, 7260−7275.
(12) Dong, H.; Dube, N.; Shu, J. Y.; Seo, J. W.; Mahakian, L. M.; Ferrara, K. W.; Xu, T. Long-Circulating 15 nm Micelles Based on Amphiphilic 3-Helix Peptide-PEG Conjugates. *ACS Nano* **2012**, *6*, 5320−5329.
(13) Shu, J. Y.; Tan, C.; DeGrado, W. F.; Xu, T. New Design of Helix Bundle Peptide - Polymer Conjugates. *Biomacromolecules* **2008**, *9*, 2111−2117.
(14) Pandey, R.; Sharma, A.; Zahoor, A.; Sharma, S.; Khuller, G. K.; Prasad, B. Poly (DL-lictide-co-glycolide) nanoparticle- Based Inhalable Sustained Drug Delivery System for Experimental Tuberculosis. *J. Antimicrob. Chemother.* **2003**, *52*, 981−986.
(15) Smyth, H. D.C.; Hickey, A. J. *Controlled Pulmonary Drug Delivery;* Springer Publisher: New York, 2011; Vol. *86*, pp 1−545.
(16) Vandal, C. H.; Nathan, C. F.; Ehrt, S. Acid Resistance in *Mycobacterium tuberculosis*. *J. Bacteriol.* **2009**, *191*, 4714−4721.
(17) Mane, S. R.; Chatterjee, K.; Dinda, H.; Das Sarma, J.; Shunmugam, R. Stimuli Responsive Nano-carrier for an Effective Delivery Multi- Frontline Tuberculosis Drugs. *Polym. Chem.* **2014**, *5*, 2725−2735.
(18) Mane, S. R.; Rao, V. N.; Chatterjee, K.; Dinda, H.; Nag, S.; Kishore, A.; Das Sarma, J.; Shunmugam, R. A Unique Polymeric Nano-carrier for Anti-tuberculosis Therapy. *J. Mater. Chem.* **2012**, *22*, 19639−19642.
(19) Grubbs, R. H. *Handbook of Metathesis;* Wiley-VCH: Weinheim, Germany, 2003; Vol. *3*, pp 1−1204.
(20) Maynard, H. D.; Sheldon, Y. O.; Grubbs, R. H. Synthesis of Norbornenyl Polymers with Bioactive Oligopeptides by Ring-Opening Metathesis Polymerization. *Macromolecules* **2000**, *33*, 6239−6242.
(21) Watson, K. J.; Park, S. J.; Im, J. H.; Nguyen, S. T. Towords Polymeric Anticancer Drug Cocktails from Ring- Opening Metathesis Polymerization. *Macromolecules* **2001**, *34*, 3507−3509.
(22) Som, A.; Tezgel, A. O.; Gabriel, G. J.; Tew, G. N. Self Activiation In De Novo Designed Mimics of Cell-Penetrating Peptides. *Angew. Chem., Int. Ed.* **2011**, *50*, 6147−6150.
(23) Mane, S. R.; Rao, V. N.; Shunmugam, R. Reversible pH- and Lipid-Sensitive Vesicles from Amphiphilic Norbornene-Derived Thiobarbiturate Homopolymers. *ACS Macro Lett.* **2012**, *1*, 482−488.
(24) Mane, S. R.; Shunmugam, R. Hierarchical Self-Assembly of Amphiphilic Homopolymer into Unique Super-structures. *ACS Macro Lett.* **2014**, *3*, 44−50.
(25) DuToit, L. C.; Pillay, V.; Danckwerts, M. P. Tuberculosis Chemotherapy: Current Drug Delivery Approaches. *Respir. Res.* **2006**, *7*, 118.
(26) Prabakaran, D.; Singh, P.; Jaganathan, K. S.; Vyas, S. P. Osmotically Regulated Asymmetric Capsular Systems for Simultaneous Sustained Delivery of Anti-Tubercular Drugs. *J. Controlled Release* **2004**, *95*, 239−248.
(27) Mane, S. R.; Rao, V. N.; Chatterjee, K.; Dinda, H.; Nag, S.; Kishore, A.; Das Sarma, J.; Shunmugam, R. Amphiphilc Homopolymer Vesicles as Unique Nano-Carriers for Cancer Therapy. *Macromolecules* **2012**, *45*, 8037−8042.